MATHEMATICAL MODELING AND COMPUTING, Vol. 8, No. 3, pp. 391–399 (2021)

Modeling Computing Mathematical

Modeling the reinforced concrete shell with a protective structure

Karhut I. I., Krochak O. V., Maksimovich S. B.

Lviv Polytechnic National University,
12 S. Bandera Str., 79013, Lviv, Ukraine

(Received 22 March 2021; Revised 30 April 2021; Accepted 3 May 2021)

The results of the mathematical modeling and experimental studies for the stress-strain state of the annular section of the reinforced concrete shell with the protective structure are presented. Computer simulation has been formulated as a stationary temperature problem. The distribution of deformations and stresses is shown using the equations of the elastic theory. A comparison of theoretical dependences on the results of experimental studies of physical models is given. Conclusions are drawn about the possibility of using them in the calculations of reinforced concrete protective structures.

Keywords: *reinforced concrete three-layer shell, elastic theory, internal pressure, temperature field, radial displacement.*

2010 MSC: 68R99, 74B05, 74F05 **DOI:** 10.23939/mmc2021.03.391

1. Introduction

The overwhelming majority of protective structures designed and built at power and other enterprises (containment shells of nuclear power plants, heat accumulators, waste storage, protective shafts, etc.) are reinforced concrete shells of circular cross-section, which are mainly vertically placed [1, 2]. Reinforcement of such type shells is adopted double with sheet outer or pre-stressed wound wire reinforcement. Full-scale tests of these structures, especially for the emergency loads combinations, are very complex and valuable, therefore, their numerical modeling and testing of physical models are carried out. The design scheme of such type structure can be represented as a three-layer shell, which is acted upon by internal pressure and elevated temperature. The stress-strain state can be determined by analyzing a three-layer plane ring as a fragment of a cylindrical shell [3] in the case for a three-layer reinforced concrete rotation shell of the enclosing structure and given external influences that satisfy the conditions of the plane problem.

2. Math modeling

Figure 1 shows the design diagram of the plane stationary problem of thermo-elasticity for a three-layer (three-component) ring, as well as for the plane problem of the elastic theory for this region. The designations adopted for a three-layer hollow long cylinder with an axisymmetric temperature field are the next: R_0 is the radius of the inner contour L_0; R_1 is the radius of the contour L_1 at the border of the first and second layers; R_2 is the radius of the contour L_2 between the second and the third layers; R_3 is the radius of the outer contour; T, T_3 are known temperatures on the inner and outer edges of the cylinder.

The conditions of ideal thermal contact (equality of temperatures and heat fluxes) are set along the contours L_1 and L_2.

Let us write down the heat conduction equations for a three-layer ring, applying the relative coordinate $\rho = \frac{R}{R_3}$ and boundary conditions:

$$\frac{d^2 t_i}{d\rho^2} + \frac{1}{\rho}\frac{dt_i}{d\rho} = 0 \qquad (i = 1, 2, 3), \tag{1}$$

$$\begin{aligned} t_1 &= T_0 && \text{at} && \rho = \rho_0, \\ t_3 &= T_3 && \text{at} && \rho = 1, \\ t_1 &= T_2 && \text{at} && \rho = \rho_1, \\ \lambda_1 \frac{dt_1}{d\rho} &= \lambda_2 \frac{dt_2}{d\rho} && \text{at} && \rho = \rho_1, \\ t_2 &= t_3 && \text{at} && \rho = \rho_2, \\ \lambda_2 \frac{dt_2}{d\rho} &= \lambda_3 \frac{dt_3}{d\rho} && \text{at} && \rho = \rho_2, \end{aligned} \tag{2}$$

where $t_i(\rho)$, λ_i is the temperature, the thermal conductivity of the i-th layer.

$$\rho_0 = \frac{R_0}{R_3}, \quad \rho_1 = \frac{R_1}{R_3}, \quad \rho_2 = \frac{R_2}{R_3}.$$

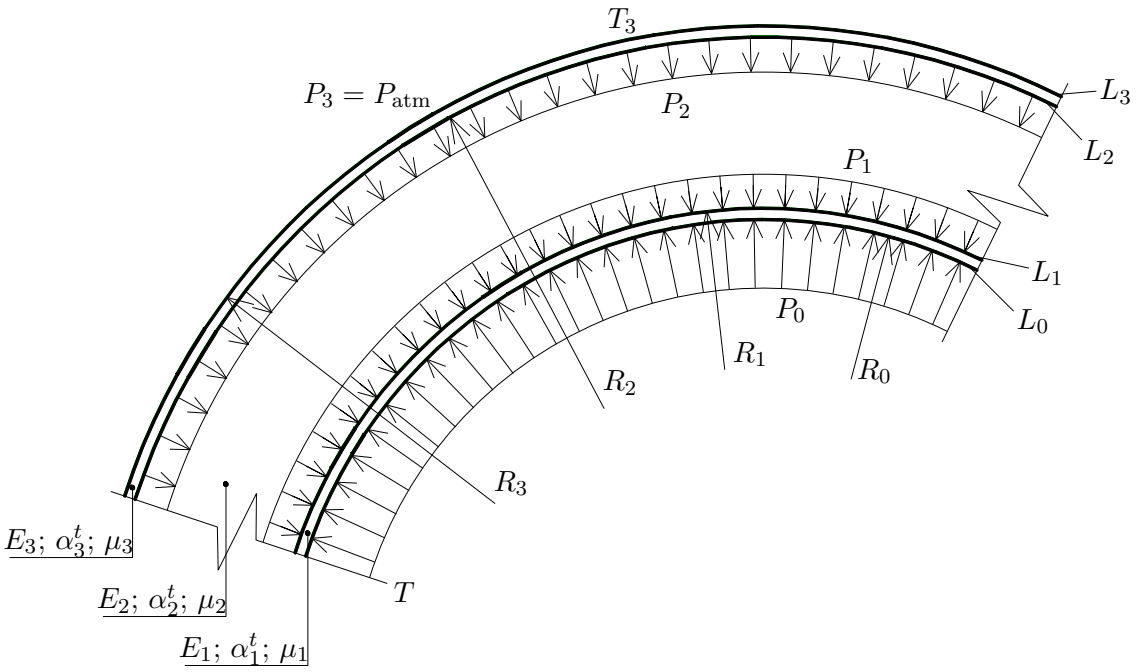

Fig. 1. Design scheme of a three-layer ring under the action of the internal pressure and the elevated temperature.

The solution to equation (1) is represented as

$$t_i(\rho) = A_i + B_i \ln \rho \qquad (i = 1, 2, 3). \tag{3}$$

Integration constants A_i and B_i can be obtained from conditions (2).

$$\begin{cases} A_1 = T_0 - \dfrac{(T_3 - T_0)\ln \rho_0}{\rho}, \quad B_1 = \dfrac{T_3 - T_0}{\rho}, \\ A_2 = T_0 - \dfrac{(T_3 - T_0)\ln \rho_0 \left(\frac{\lambda_1}{\lambda_2} - \frac{\lambda_2}{\lambda_3}\right) \ln \rho_2}{\rho}, \\ B_2 = \dfrac{\lambda_1}{\lambda_2} \dfrac{(T_3 - T_0)\ln \rho_0}{\rho}, \\ A_3 = T_3, \quad B_3 = \dfrac{\lambda_1}{\lambda_3} \dfrac{(T_3 - T_0)\ln \rho_0}{\rho}, \end{cases} \tag{4}$$

where

$$\rho = \left(\frac{\lambda_1}{\lambda_2} - \frac{\lambda_2}{\lambda_3}\right)\ln\rho_2 + \left(1 - \frac{\lambda_1}{\lambda_2}\right)\ln\rho_1 - \ln\rho_0.$$

Substituting (4) into (3), one can obtain the equation for the temperature distribution over the thickness of the three-layer ring for the given boundary conditions (2) and the ideal thermal contact of the layers:

$$T_1(\rho) = T_0 - \frac{(T_3 - T_0)\ln\rho_0}{\rho} + \frac{(T_3 - T_0)}{\rho}\ln\rho \tag{5}$$

$$T_{11}(\rho) = T_0 - \frac{(T_3 - T_0)\ln\rho_0\left(\frac{\lambda_1}{\lambda_2} - \frac{\lambda_2}{\lambda_3}\right)\ln\rho_2}{\rho} + \frac{\lambda_1}{\lambda_2}\frac{(T_3 - T_0)\ln\rho_0}{\rho}\ln\rho, \tag{6}$$

$$T_{111}(\rho) = T_3 + \frac{\lambda_1}{\lambda_3}\frac{(T_3 - T_0)\ln\rho_0}{\rho}\ln\rho. \tag{7}$$

To determine the temperature stresses in a three-layer ring (a fragment of a long cylinder), the known temperature field from the heat conduction problem under the accepted boundary conditions (2) is used.

Let us write the equations for the radial and ring stresses and displacements of the three layers of the ring in the general form via the polar coordinates:

$$\sigma_r^V = C_V + \frac{D_V}{\rho^2} - \frac{\alpha_V^{t'}E_V'}{\rho^2}\int_{\rho_V}^{\rho} t_V(\rho)\,\rho\,d\rho \qquad (V = 1, 2, 3), \tag{8}$$

$$\sigma_\theta^V = C_V - \frac{D_V}{\rho^2} - \alpha_V^{t^1}E_V^1 t_V(\rho) + \frac{\alpha_V^{t^1}E_V^1}{\rho^2}\int_{\rho_1}^{\rho} t_V(\rho)\,\rho\,d\rho, \tag{9}$$

$$u_r^V = \left(\frac{1}{E_V^1}\left(\left(\sigma_\theta^V - \mu_V^1\sigma_r^V\right) + \alpha_V^{t^1}t_V(\rho)\right)R\right), \tag{10}$$

where

$$\mu_i^{'} = \frac{\mu_i}{1 - \mu_i}, \quad E_i^{'} = \frac{E_i}{1 - \mu_i^2}, \quad \alpha_V^{t^1} = \alpha_V^t(1 - \mu_V), \tag{11}$$

E_i, α_i^t, μ_i are the elasticity modulus, temperature coefficient of the linear expansion, Poisson's ratio for the layers of the cylinder, respectively.

If there is no external load on all circuits L_0, L_1, L_2, L_3, then the integration constants C_i, D_i $(i = 1, 2, 3)$ are determined from the conditions:

$$\begin{cases} \sigma_r^1 = 0 & \text{at} \quad \rho = \rho_0, \\ \sigma_r^3 = 0 & \text{at} \quad \rho = 1, \\ \sigma_r^3 = \sigma_r^2 & \text{at} \quad \rho = \rho_1, \\ u_r^1 = u_r^2 & \text{at} \quad \rho = \rho_1, \\ u_r^2 = u_2^3 & \text{at} \quad \rho = \rho_2, \end{cases} \tag{12}$$

Substituting (8), (9), (10) into (12), we obtain

$$\begin{cases} C_1 = \left(F_1 + \frac{F_2}{\rho_1^2} + a_{01}\right)\frac{\rho_1^2}{\rho_1^2 - \rho_0^2}, \\ C_2 = F_1, \quad C_3 = a_{21} - \left(F_1 + \frac{F_2}{\rho_2^2} - a_{12} - a_{21}\right)\frac{\rho_2^2}{\rho_2^2}, \\ D_2 = F_2, \quad D_1 = -\left(a_{01} + \left(F_1 + \frac{F_2}{\rho_1^2}\right)\right)\frac{\rho_0^2\rho_1^2}{\rho_1^2 - \rho_0^2}, \\ D_3 = \left(F_1 + \frac{F_2}{\rho_2^2} - a_{12} - a_{21}\right)\frac{\rho_2^2}{1 - \rho_2^2}, \end{cases} \tag{13}$$

where

$$F_1 = \frac{\rho_2 x_2 - \rho_1 y_2}{y_1 x_2 - y_2 x_1}, \quad F_2 = \frac{\rho_2 x_1 - \rho_1 y_1}{y_1 x_2 - y_2 x_1},$$

$$x_1 = \frac{1}{E_2}\left(1-\mu_2^1\right) - \frac{1}{E_3}\left(1 - \frac{2}{\rho_2^2-1} - \mu_3^1\right),$$

$$x_2 = \frac{1}{\rho_2}\left(\frac{1}{E_2}\left(1+\mu_2^1\right) + \frac{1}{E_3}\left(1 - \frac{2}{\rho_2^2-1} - \mu_3^1\right)\right),$$

$$y_1 = \frac{1}{E_2}\left(1 - \frac{\rho_0^2}{\rho_0^2-\rho_1^2} - \mu_2^1\right) - \frac{1}{E_3}\left(1-\mu_2^1\right),$$

$$y_2 = \frac{1}{\rho_1^2}\left(\frac{1}{E_2}\left(-1 + \frac{\rho_0^2}{\rho_0^2-\rho_1^2} + \mu_2^1\right) + \frac{1}{E_3}\left(1 - \frac{2}{\rho_2^2-1} - \mu_3^1\right)\right),$$

$$P_1 = \frac{1}{E_2}\left(a_{22}^1 - a_{12}\left(\mu_2^1+1\right)\right) + \frac{1}{E_3}\left(\frac{2\left(a_{21}+a_{12}\right)}{\rho_2^2-1} - a_{12}\left(1+\mu_3^1\right) - a_{33}\right) + b_{33} - b_{22}^1,$$

$$P_2 = \frac{1}{E_1}\left(\frac{2a_{01}\rho_0^2}{\rho_0^2-\rho_1^2} + a_{11} - 2a_{01}\right) - \frac{1}{E_2}a_{22} + b_{22} - b_{11}.$$

Substituting (13) into (8), (9) and considering:

$$\begin{cases} \displaystyle\int_{\rho_0}^{\rho} t_1(\rho)\,\rho\,d\rho = \frac{1}{2}A_1\left(\rho^2-\rho_0^2\right) + \frac{1}{2}B_1\left(\rho^2\ln\rho - \rho_0^2\ln\rho_0 - \frac{1}{2}\left(\rho^2-\rho_0^2\right)\right), \\ \displaystyle\int_{\rho_1}^{\rho} t_2(\rho)\,\rho\,d\rho = \frac{1}{2}A_2\left(\rho^2-\rho_1^2\right) + \frac{1}{2}B_2\left(\rho^2\ln\rho - \rho_1^2\ln\rho_1 - \frac{1}{2}\left(\rho^2-\rho_1^2\right)\right), \\ \displaystyle\int_{\rho_2}^{\rho} t_3(\rho)\,\rho\,d\rho = \frac{1}{2}A_3\left(\rho^2-\rho_2^2\right) + \frac{1}{2}B_3\left(\rho^2\ln\rho - \rho_2^2\ln\rho_2 - \frac{1}{2}\left(\rho^2-\rho_2^2\right)\right), \end{cases} \tag{14}$$

$$a_{01} = \frac{\alpha_1^{t'}E_1}{\rho_1^2}\int_{\rho_0}^{\rho_1} t_1(\rho)\,\rho\,d\rho = \frac{\alpha_1^{t'}E_1^1}{\rho_1^2}\left(\frac{1}{2}A_1\left(\rho_1^2-\rho_0^2\right) + \frac{1}{2}B_1\left(\rho_1^2\ln\rho_1 - \rho_0^2\ln\rho_0 - \frac{1}{2}\left(\rho_1^2-\rho_0^2\right)\right)\right),$$

$$a_{12} = \frac{\alpha_2^{t'}E_2}{\rho_0^2}\int_{\rho_1}^{\rho_2} t_2(\rho)\,\rho\,d\rho = \frac{\alpha_2^{t'}E_2^1}{\rho_2^2}\left(\frac{1}{2}A_2\left(\rho_2^2-\rho_1^2\right) + \frac{1}{2}B_2\left(\rho_2^2\ln\rho_2 - \rho_1^2\ln\rho_1 - \frac{1}{2}\left(\rho_2^2-\rho_1^2\right)\right)\right),$$

$$a_{21} = \alpha_3^{t'}E_3^1\int_{\rho_2}^{1} t_3(\rho)\,\rho\,d\rho = \alpha_3^{t'}E_3^1\left(\frac{1}{2}A_3\left(1-\rho_2^2\right) - \frac{1}{2}B_2\left(\rho_2^2\ln\rho_2 + \frac{1}{2}\left(1+\rho_2^2\right)\right)\right),$$

$$a_{11} = \alpha_1^{t'}E_2^1 t_2(\rho) = \alpha_2^{t'}E_2^2\left(A_2 + B_2\ln\rho_1\right) \quad \text{at} \quad \rho=\rho_1,$$

$$a_{22} = \alpha_2^{t'}E_2^1 t_2(\rho) = \alpha_2^{t'}E_2^1\left(A_2 + B_2\ln\rho_2\right) \quad \text{at} \quad \rho=\rho_2,$$

$$a_{22}^1 = \alpha_2^{t'}E_2^1 t_2(\rho) = \alpha_2^{t'}E_2\left(A_2 + B_2\ln\rho_2\right) \quad \text{at} \quad \rho=\rho_2,$$

$$a_{33} = \alpha_3^{t'}E_3^1 t_3(\rho) = \alpha_3^{t'}E_3^1\left(A_3 + B_3\ln\rho_2\right) \quad \text{at} \quad \rho=\rho_2,$$

$$b_{11} = \alpha_1^{t'}t_1(\rho) = \alpha_1^{t'}\left(A_1 + B_1\ln\rho_1\right) \quad \text{at} \quad \rho=\rho_1,$$

$$b_{22} = \alpha_1^{t'}t_2(\rho) = \alpha_2^{t'}\left(A_2 + B_2\ln\rho_1\right) \quad \text{at} \quad \rho=\rho_1,$$

$$b_{22}^1 = \alpha_2^{t'}t_2(\rho) = \alpha_2^{t'}\left(A_2 + B_2\ln\rho_2\right) \quad \text{at} \quad \rho=\rho_2,$$

$$b_{33} = \alpha_3^{t'}t_3(\rho) = \alpha_3^{t'}\left(A_3 + B_3\ln\rho_2\right) \quad \text{at} \quad \rho=\rho_2.$$

Finally, we find the value of the temperature stresses in each of the three layers σ_r^i, σ_θ^i and the radial displacement in a thin three-layer ring at a plane stress state determined by the plane force and temperature field, replacing the values of E_V^1, α_V^{t1}, μ_V^1 with E_V, α_V^t, μ_V.

Let us find the stresses in the three-layer ring from the internal normal uniformly distributed pressure p_0 on the contour L_0. In this case, contact pressures p_1 act on the rings boundaries (from the side of the II ring on the I ring along the contour L_1) and p_2 (from the side of the III ring on the II ring along the contour L_2). The pressures p_1 and p_2 are opposite in direction to the outer normals.

To determine the contact pressures p_1 and p_2, we write down a system of two equations:

$$\begin{cases} a_1p_1 + a_2p_2 = a_3, \\ b_1p_1 + b_2p_2 = 0, \end{cases} \tag{15}$$

where

$$\begin{cases} a_1 = a_4\left(R_1^2\left(1-\mu_1'\right) + R_0^2\left(1+\mu_1'\right)\right) - \left(R_1^2\left(1-\mu_2'\right) + R_2^2(1+\mu_0')\right), \\ a_2 = -2R_2^2a_4 = \dfrac{E_2'\left(R_2^2-R_1^2\right)}{E_1'\left(R_1^2-R_2^2\right)}a_3 = 2a_4\rho_0R_0^2, \\ b_1 = 2b_4R_1^2b_2 = R_2^2\left(1-\mu_3'\right) + R_3^2\left(1+\mu_3'\right) + b_4\left(R_2^2(1-\mu_2') + R_1^2\left(1+\mu_2'\right)\right), \\ b_4 = -\dfrac{E_3'\left(R_3^2-R_2^2\right)}{E_2'\left(R_2^2-R_1^2\right)}. \end{cases} \tag{16}$$

The solution to system (15) according to Cramer's rule is:

$$p_1 = \frac{\Delta p_1}{\Delta}, \qquad p_2 = \frac{\Delta p_2}{\Delta},$$

where $\Delta = \begin{vmatrix} a_1a_2 \\ b_1b_2 \end{vmatrix} = a_1b_2 + b_1a_2$, $\Delta p_1 = a_3b_2$, $\Delta p_2 = -a_3b_1$.

To pass to the case of plane deformation, the replacement of the quantities μ_i and E_i by the quantities $\mu_i' = \frac{\mu_i}{1-\mu_i}$, $E_i' = \frac{E_i}{1-\mu_i^2}$ $(i = 1, 2, 3)$ is used.

For the first layer:

$$\sigma_r^1 = \frac{p_0R_0^2(R^2-R_1^2) - p_1R_1^2(R^2-R_0^2)}{R^2(R_1^2-R_0^2)}, \tag{17}$$

$$\sigma_\theta^1 = \frac{p_0R_0^2(R^2+R_1^2) - p_1R_1^2(R^2+R_0^2)}{R^2(R_1^2-R_0^2)} \quad (R_0 < R < R_1), \tag{18}$$

where σ_r, σ_θ are normal radial and hoop stresses.

For the second layer:

$$\sigma_r^{11} = \frac{-p_1R_1^2(R^2-R_2^2) - p_2R_2^2(R^2-R_1^2)}{R(R_2^2-R_1^2)}, \tag{19}$$

$$\sigma_\theta^{11} = \frac{-p_1R_1^2(R^2+R_2^2) - p_2R_2^2(R^2+R_1^2)}{R^2(R_2^2-R_1^2)} \quad (R_1 < R < R_2). \tag{20}$$

For the third layer:

$$\sigma_r^{111} = \frac{-p_2R_2^2(R^2-R_3^2)}{R^2(R_3^2-R_2^2)}, \tag{21}$$

$$\sigma_\theta^{111} = \frac{-p_2R_2^2(R^2+R_3^2)}{R^2(R_3^2-R_2^2)} \quad (R_2 < R < R_3). \tag{22}$$

Let us also find the radial displacement u_r^i in a thin three-component ring in a plane stressed state determined by a plane force and temperature field. The boundary conditions (12) with an ideal contact specified on the contours L_1 and L_2, and Hooke's law are used for a plane stress state in the next form:

$$u = \frac{R}{E}\left(\sigma_\theta - \mu\sigma_r\right) \tag{23}$$

The validity of which for the second concrete ring is determined by the restrictions imposed on the protective structure – $(\sigma_b \leqslant 0.3f_{cd})$ the work of the structure in the elastic stage ensures the absence of not only macro, but also microcracks [7].

Dependencies for determining the stresses and displacements of the ring are conveniently calculated using computer programs. The principle of superposition is used to determine the stresses under the combined action of the internal pressure and the temperature field.

3. Computer modeling

Computer modeling. Using the LIRA 10.8 software package (release 3.4), in the formulation of a stationary temperature problem, the case with an uninsulated outer face of a three-layer ring was considered (the problem "ring 1.68", Fig. 2). The radial displacements of the numerical model of such type ring (expansion) at the $p_0 = 1.68$ MPa were $1.5 - 2$ times less than those obtained experimentally and calculated in an elastic formulation and with the use of a deformable model. This indicates a significant effect of the temperature of the sheet reinforcement on the outer face on the deformability.

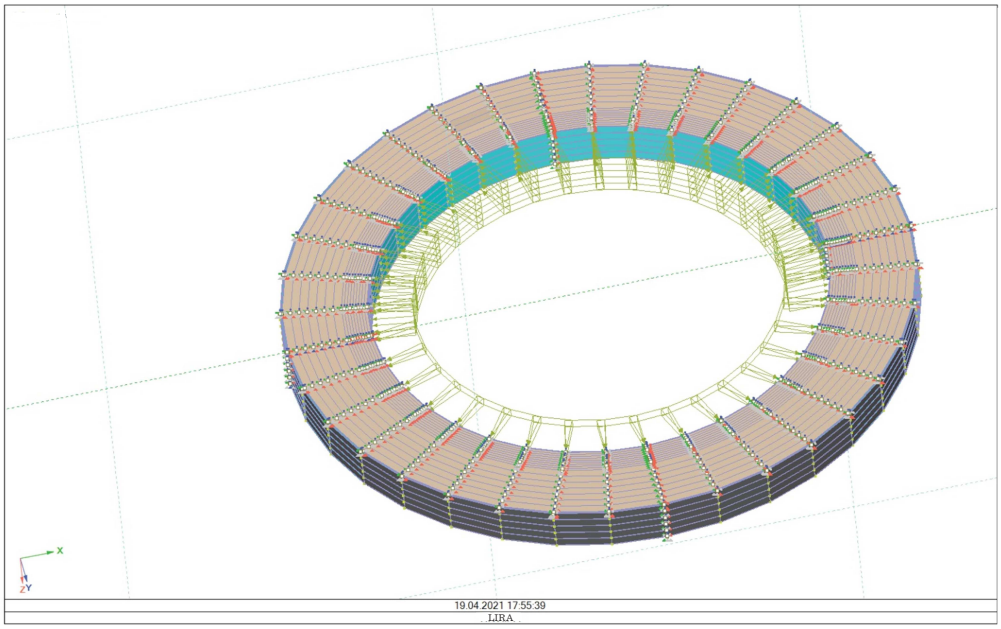

Fig. 2. Simulation of thermal power loads on a three-layer reinforced concrete ring with sheet reinforcement (external temperature 18°C.

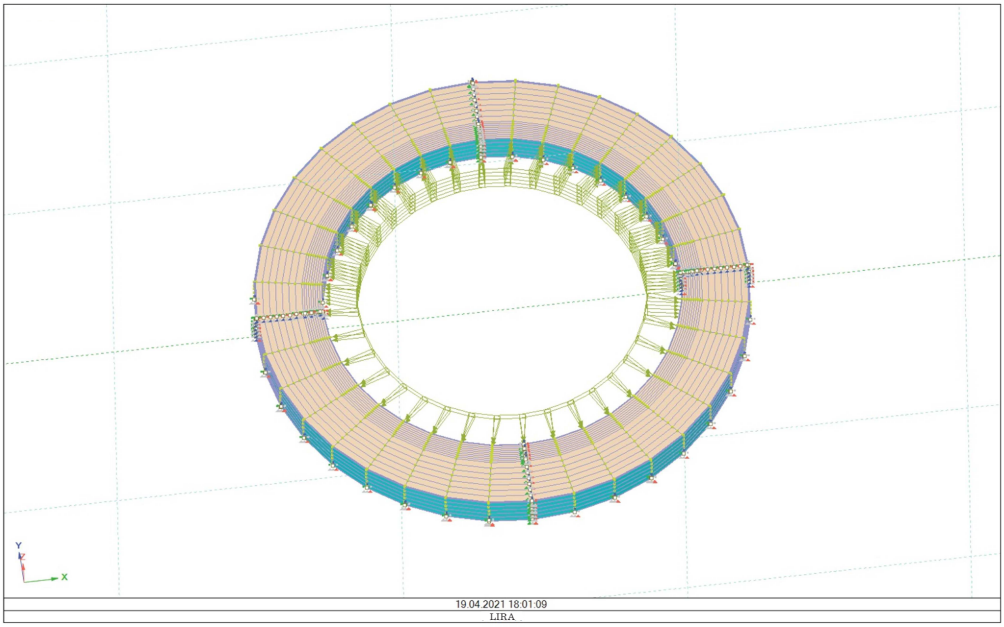

Fig. 3. Modeling of thermal power loads on a three-layer reinforced concrete ring with sheet reinforcement (internal temperature 240°C, external temperature 180°C).

At $p_0 = 3.2$ MPa and when the yield stress in the reinforcement is reached, this difference remains. When insulating the outer face (Fig. 3), the radial displacements of the numerical model at $p_0 =$

1.68 MPa were 7% less than those obtained experimentally and calculated in an elastic formulation and using a deformation model.

The temperature moments, depending on the temperature difference set on the inner and outer faces of the ring in experimental studies and in the numerical experiment, coincided. These results confirmed the need to insulate the outer edge of the shells of protective structures. Modeling the distribution of principal stresses in three-layer annular specimens performed according to the theories of Huber–Genki–Mises (G-G-M), Geniev (G), Pisarenko–Lebedev (P-L) and Druckner–Prager (D-P), showed the best agreement of research results when using the latter one.

4. Analysis of research results

At the normal temperature of the outer face, the difference between the stresses in the outer steel sheet of the shell, obtained from the numerical experiment, was 9.7% (deforming model) and $5.1 - 7.3\%$ (experimental values), and for the inner steel sheet of the shell 13.4% and $0.6 - 2.0\%$, respectively, both for normal temperature and for long-term heating of the inner edge (Table 1).

Table 1. Stresses in concrete and reinforcement of three-layer rings.

Research modes	σ, MPa	Sheet corrugated			Sheet smooth			Sheet corrugated			Sheet smooth		
		exp.	theor.	num.	exp.	theor.	num.	exp.	theor.	num.	exp.	theor.	num.
Power $P = 1.68$ MPa	σ_s^1	29.8	24.9	30.4	34.9	24.9	30.4	–	–		–	–	
	σ_c	1.6	3.1	2.0	1.2	3.1	2.0	–	–		–	–	
	σ_s	32.5	19.6	30.3	34.0	19.6	30.3	–	–		–	–	
Thermopow. $P = 1.68$ MPa, $T = 240°$C	σ_s^1	–	–	–	–	–	–	34.4	44.3	39.0	35.9	44.3	39.0
	σ_c	–	–	–	–	–	–	1.72	4.02	2.88	1.53	4.02	2.88
	σ_s	–	–	–	–	–	–	33.7	39.0	31.4	34.4	39.0	31.4
Prolonged heating, $T = 240°$C	σ_s^1	13.4	21.0	15.2	14.9	21.0	15.2	–	–	–	–	–	–
	σ_c	1.12	1.84	1.66	1.02	1.84	1.66	–	–	–	–	–	–
	σ_s	15.0	24.2	16.1	15.8	24.2	16.1	–	–	–	–	–	–
Thermopow. $P = 1.68$ MPa, $T = 240°$C	σ_s^1	32.1	44.3	39.0	33.9	44.3	39.0	35.0	44.3	39.0	38.6	44.3	39.0
	σ_c	1.65	4.02	2.88	1.26	4.02	2.88	1.78	4.02	2.88	1.42	4.04	2.88
	σ_s	34.4	39.0	31.4	35.8	39.0	31.4	36.0	39.0	31.4	37.3	39.0	31.4

Note: theoretical values in accordance with dependencies (18), (20), (22), numerical according to LIRA 10.8 (release 3.4, D-P theory).

Table 2. Radial displacements of the outer face of three-layer rings f, mm.

Type of reinforcement	Test modes, T on the inner edge	Internal pressure p_0, MPa	Experiment, physical model	Theoretical by (23) and (10)	Numerical experiment, Drucker–Prager theory
smooth sheet	power	1.68	0.077	0.068	0.099
	$T = 18°$C	3.2	0.146	0.129	0.189
	thermo power	1.68	1.93	1.88	1.78
	$T = 240°$C short-term	3.2	3.67	3.02	1.90
	thermo power	1.68	2.17	–	–
	$T = 240°$C long-term	3.2	4.18	–	–
corrugated sheet	power	1.68	0.063	0.063	0.099
	$T = 18°$C	$p_0 = 3.2$	0.121	0.120	0.189
	thermo power	$p_0 = 1.68$	1.49	1.76	1.65
	$T = 240°$C short-term	$p_0 = 3.2$	2.84	2.82	1.78
	thermo power	1.68	1.68	–	–
	$T = 240°$C long-term	3.2	3.22	–	–

The obtained deviations indicate a good convergence of the experimental results with the results of a numerical experiment, reflecting the distribution of stresses between the inner and outer shell sheets.

Table 2 shows the displacements of the outer face of the three-layer ring obtained in numerous and physical experiments, and a comparison with the obtained theoretical dependences of the elastic theory.

The obtained theoretical dependences (18), (20), (22), (23) for stresses and strains were compared with the results of experimental studies of three-layer annular models [4, 6] and experimental studies of V. A. Kostornichenko [8] (Table 3 and Table 5). Consequently, using the provisions of the elastic theory and at $p_0 \leqslant 0,4p_u$, which corresponds to the constraints imposed on the structure, ensures a

good convergence of the results and the discrepancy does not exceed 7%. The tensile bearing capacity of the ring elements is determined by the bearing capacity of the reinforcement. Comparison of the theoretical and experimental results of the study of the tensile bearing capacity of ring sections is shown in Table 4. The discrepancy does not exceed $4 - 12\%$.

Table 3. Moments of cracking in three-layer rings.

Type of reinforcement	T, °C	p_{crc} (MPa)	M_{crc} (kNm)	M_{crc} (kNm)	M_{exp}/M_{theor}
Smooth sheet	18	0.21	9.05	8.70	1.04
Corrugated sheet	18	0.42	17.62	16.62	1.06
Smooth sheet	240		2.73	2.65	1.03
Corrugated sheet	240		3.12	3.03	1.03
Bar of period. profile	18	0.194*	8.32*	8.15	1.021
Bar of period. profile	150	–	2.36**	2.21	1.067

T is the temperature of the inner face, * theoretical value according to [9], ** experimental research of Kostornichenko V. A. [8].

Table 4. Tensile bearing capacity of three-layer rings during short-term thermo-power tests.

Type of reinforcement of samples	T, °C	Ultimate tensile force N, kN		N_{exp}/N_{theor}
		exp.	theor.	
Corrugated sheet	18	407.1	387.7	1.05
Smooth sheet	18	383.2	351.6	1.09
Corrugated sheet	240	370.85	356.27	1.04
Smooth sheet	240	380.1	348.5	1.09
Bar of period. profile	18	149.78*	133.37	1.12
Bar of period. profile	150	140.33*	127.56	1.10

* experimental research Kostornichenko V. A. [8].

Table 5. Temperature moments in three-layer rings at different heating modes (kNm).

Temperature mode	Experimental values			Theoretical values according to [9]	M_{exp}/M_{theor}
	Corrugated sheet	Smooth sheet	Bar of period. profile		
First short-term heating up to 240°C	6.1	6.5	–	6.2	1.03
Long-term heating up to 240°C	1.05	1.2	–	1.11	1.01
Short-term heating up to 150°C	–	–	3.07	3.24	0.96
Long-term heating up to 150°C	–	–	0.25	0.27	0.93

* experimental research Kostornichenko V. A. [8].

In case when the loads are close to the limiting state, the convergence of results is much better in contrast to using the deformable model adopted in the current standards [5,10] and taking into account the real deformation diagrams of concrete and reinforcement [9, 11, 12] (Table 5). The discrepancy does not exceed 7%. The nonlinear deformable model reliably describes the processes occurring in the structure, and allows to unambiguously determine its stress-strain state until the limit state is reached.

5. Conclusions

The carried out theoretical, experimental studies and computer modeling of the reinforced concrete three-layer annular fragments of protective structures have shown the possibility of using the dependences of the elastic theory and existing algorithms in the formulation of a stationary thermo-elastic problem to determine with high accuracy the stress-strain state of specimens in the mode of stationary long-term heating (operational thermal power loads).

Numerical experiments carried out using the deformable model and the provisions of the Druckner–Prager theory showed the slightest deviations from those obtained experimentally. The deviation did not exceed $2.4 - 5.8\%$.

The stresses and displacements in a three-layer annular fragment, being obtained in the numerical experiments on force loads at the normal temperature and thermal power loads in the formulation of the stationary thermo-elastic problem, demonstrate good agreement with the results of the experimental studies on the models under operational loading. The deviation did not exceed 7%.

The nonlinear deformation model adopted in the current standards, taking into account the real deformation diagrams of concrete and reinforcement, reliably describes the processes occurring in the

structure, and allows to unambiguously determine its stress-strain state in the limiting state. The discrepancy does not exceed 7%.

[1] C.T.I.C.M. Methode de prevision par le calcul du comportement au feu des structures en acier. Revue Construction Metallique. N4, 1976, p.33–40.

[2] Klimenko F., Gawrylak A., Karhoot I. Stalowobetonowe konstrukcje powlok w budownictwe energetycznym. Inzynieria i budownictwo. **8**, 469–470 (1996), (in Polish).

[3] Nalimov V. V. Teorija eksperimenta. Moskva (1971), (in Russian).

[4] Karkhut I. I. Temperaturni navantazhennia na zalizobetonni zakhysni konstruktsii. Lviv, Lviv Polytechnic National University (2015), (in Ukrainian).

[5] DBN V.2.6-98-2009. Betonni ta zalizobetonni konstruktsii. Osnovni polozhennia (in Ukrainian).

[6] Karhut I. I., Prokopchuk I. V., Gavriljak A. I., Luchko I. I. Eksperimental'nye issledovanija stalebetonnyh kolec na silovoe vozdejstvie. Visnyk LPI: "Rezervy progressa v arhitekture i stroitel'stve". **243**, 36–37 (1990), (in Russian).

[7] Berg O. Ja. Fizicheskie osnovy teorii prochnosti betona i zhelezobetona. Moskva, Gosstrojizdat (1962), (in Russian).

[8] Kostornichenko V. A. Prochnost', deformativnost' i treshhinostojkost' zhelezobetonnyh kol'cevyh jelementov pri vozdejstvii temperaturnogo perepada v diapazone $-50°C + 150°C$ i vnutrennego davlenija. Dis.... kand. tehn. nauk. Moskva (in Russian).

[9] Krichevskij A. P., Korsun V. I. Prochnost' i deformacii tjazhelogo betona v uslovijah ploskogo naprjazhennogo sostojanija pri dejstvii temperatur. V Sb. Raschet, proektirovanie i ispytanie zhelezobetonnyh konstrukcij, prednaznachennyh dlja jekspluatacii v uslovijah suhogo zharkogo klimata. Tashkent. 100–104 (1985), (in Russian).

[10] DSTU B V.2.6-156-2010 Betonni ta zalizobetonni konstruktsii z vazhkoho betonu (in Ukrainian).

[11] Krochak O. V. Raschet stalebetonnyh izgibaemyh jelementov s ispol'zovaniem real'nyh diagramm deformirovanija betona i armatury. Mehanika i fizika razrushenija kompozitnyh materialov i konstrukcij: Tez. dokl. 1 Vsesojuznogo simpoziuma. Uzhgorod. 44–45 (1988), (in Russian).

[12] Bambura A. M. Eksperymentalni osnovy prykladnoi deformatsiinoi teorii zalizobetonu: avtoref. dys. na zdobuttia stupenia d-ra tekhn. nauk: spets. 05.23.01 "Budivelni konstruktsii, budivli ta sporudy". KhDTUBA. Kharkiv (2006), (in Ukrainian).

Моделювання залізобетонної оболонки захисної споруди

Кархут І. І., Крочак О. В., Максимович С. Б.

Національний університет "Львівська політехніка",
вул. С. Бандери, 12, 79013, Львів, Україна

Наведено результати математичного моделювання та експериментальних досліджень напружено-деформованого стану кільцевого перерізу залізобетонної оболонки захисної споруди. Виконано комп'ютерне моделювання в постановці стаціонарної температурної задачі. Показано розподіл деформацій та напружень при застосуванні рівнянь теорії пружності. Наведено порівняння теоретичних залежностей з результатами експериментальних досліджень фізичних моделей та зроблено висновки про можливість застосування їх при розрахунках залізобетонних захисних споруд.

Ключові слова: *залізобетонна тришарова оболонка, теорія пружності, внутрішній тиск, температурне поле, радіальне переміщення.*